

# Production of *Dynamic Frozen Waves*: Controlling shape, location (and speed) of diffraction-resistant beams <sup>(†)</sup>

Tárcio A. Vieira <sup>1,3</sup>, Marcos R.R. Gesualdi <sup>1</sup>, Michel Zamboni-Rached <sup>2,4</sup>, and Erasmo Recami <sup>2,5,6</sup>

<sup>1</sup> *Universidade Federal do ABC, Santo André, SP, Brazil.*

<sup>2</sup> *University of Campinas, Campinas, SP, Brazil.*

<sup>3</sup> *University of Sao Carlos, Sao Carlos, SP, Brazil.*

<sup>4</sup> *University of Toronto, Toronto, Canada.*

<sup>5</sup> *University of Bergamo, Bergamo, Italy.*

<sup>6</sup> *INFN-Sezione di Milano, Milan, Italy.*

**Abstract** — In recent times, we experimentally realized a quite efficient modeling of the shape of diffraction-resistant optical beams; thus generating for the first time the so-called *Frozen Waves* (FW), whose longitudinal intensity pattern can be arbitrarily chosen, within a prefixed space interval of the propagation axis. Such waves possess a host of potential applications: in medicine, biomedical optics, optical tweezers, atom guiding, remote sensing, tractor beams, optical communications or metrology, and other topics in photonic areas. In this work, we extend our theory of FWs—which led to beams endowed with a *static* envelope—through a *dynamic* modeling of the FWs, whose shape is now allowed to evolve in time in a predetermined way. And we experimentally create such dynamic FWs in Optics, via a computational holographic technique and a spatial light modulator. Experimental results are here presented for two cases of dynamic FWs, one of the zeroth and the other of higher order, the last one being the most interesting, consisting in a cylindrical surface of light whose geometry changes in space and time.

PACS nos.: 42.25.Bs; 42.25.Fx; 41.20.Jb; 46.40.Cd; 41.85.-p; 46.40.Cd; 42.20.Ht; 42.40.Jv, 42.30.Lr.

*1. Introduction* — The “Frozen Waves” (FWs)[1, 2, 3] are very peculiar solutions to the wave equations consisting in non-diffracting beams whose longitudinal intensity pattern can be freely chosen within a prefixed space interval  $0 \leq z \leq L$  of the propagation axis. For such beams even a certain degree of control on their transverse intensity pattern is possible. This endows the FW-type beams with a great deal of potential applications, since the concrete possibility of modeling their spatial intensity shape *adds* to the exceptional characteristic of all the “Localized Waves”, or Non-Diffracting Waves (NDW), of resisting the effects of diffraction[4, 5, 6].

The theoretical development of FWs can be found in Refs.[1, 2, 3, 7], besides in the above-quoted reviews or books: We call it, briefly, the FW method. Synthesizing, a FW is a superposition of co-propagating and equal-frequency *Bessel beams* (of zeroth or higher order)

$$\Psi(\rho, \phi, z, t) = \mathcal{N}_\nu e^{-i\omega t} \sum_{n=-N}^N A_n J_\nu(k_{\rho n} \rho) e^{ik_{zn} z} e^{i\nu \phi}, \quad (1)$$

with  $\mathcal{N}_\nu = 1/[J_\nu(\cdot)]_{max}$ , where  $[J_\nu(\cdot)]_{max}$  is the maximum value of the Bessel function of the first kind  $J_\nu(\cdot)$ ;  $k_{\rho n}$  and  $k_{zn}$  are transverse and longitudinal wave numbers of the  $n$ -th Bessel beam in the superposition, satisfying the known relation  $k_{\rho n}^2 = \omega^2/c^2 - k_{zn}^2$ . The FW method requires the longitudinal wavenumbers to be chosen so that  $k_{zn} = Q + 2\pi n/L$ , quantity  $Q$  being a constant to be selected, in the case for instance of zero order FWs, according to the desired spot-size  $\Delta\rho_0$ , besides for constructing solely (not evanescent) beams *propagating* in the positive direction. (Let us recall that a partial control on the

(†) contact: mzamboni@decom.fee.unicamp.br

beam transverse intensity too can be obtained by a suitable choice of  $Q$ , and also by having recourse to higher order Bessel beams).

An important point is that the FW method[1, 2, 3, 7] shows that, once it has been arbitrarily chosen the desired intensity longitudinal pattern  $|F(z)|^2$  in the spatial interval  $0 < z < L$ , then the coefficients in superposition (1) have to be  $A_n = (1/L) \int_0^L F(z) e^{-i \frac{2\pi}{L} n z} dz$ .

This is enough to obtain Diffraction-Resistant beams with the required longitudinal intensity pattern, concentrated: (i) either along the propagation axis ( $\rho = 0$ ), when zero-order ( $\nu = 0$ ) Bessel beams are chosen in solution (1); it is then possible to determine the spot radius of the resulting beam from the parameter  $Q$  via the relation  $Q = (\omega^2/c^2 - 2.4^2/\Delta\rho_0^2)^{1/2}$ ; (ii) or over a cylindrical surface, if a positive integer is adopted for  $\nu$  in (1); in which case, the cylinder radius can be approximately evaluated through the equation  $[(d/d\rho)J_\nu(\rho\sqrt{\omega^2/c^2 - Q^2})]_{\rho=\rho_0} = 0$ .

It should be stressed that optical FWs have been concretely generated via computational holography: see Refs.[8, 9]; without forgetting that ultrasonic FWs have been reproduced also in Acoustics, at least by simulated experiments[10]. The experimental production of the FWs opened the door to a great deal of applications in a number of different areas: like medicine, biomedical optics, optical tweezers, atom guiding, remote sensing, tractor beams, optical communications or metrology, and so on.

Before going on, let us recall that FWs belong to the set of the subluminal NDWs, corresponding to the very particular case of zero peak-velocity[11, 12]: They possess, indeed, a *static* envelope (within which only the carrier wave propagates)[1, 2, 3]. It appears convenient, however, investigating, and constructing dynamic FWs, for all applications in which a traveling FW appears to be desirable and useful. Aim of this work is just extending the FW method towards a dynamic modeling of the non-diffracting beams, whose shape can slightly evolve in time in a predetermined way. That is, now we want our resulting non-diffracting beams to be endowed with a spatial shape which changes in time, as requested by the particular application considered; and to produce experimentally such dynamic FWs in Optics, via a computational holographic technique[8, 9, 13, 14] in which computer generated holograms of the FWs are created, as specified below, and then reproduced by use of a spatial light modulator (SLM). [Such a resulting wave, that corresponds to an intensity pattern no longer static, and slightly loses therefore its monochromaticity, could not be called a beam, strictly speaking...: However, if we consider the time evolution of its shape much slower than the period associated to the relevant frequency, our approach ends constituting an excellent approximation].

In equation (1) we need inserting the time dependence, first, of the coefficients  $A_n$ , and, second, of the parameter  $Q$  which enters the definition of the wavenumbers. Once it has been chosen the desired longitudinal intensity  $|F(z, t)|^2$ , one can exploit *the way* the said temporal variations are implemented, so as to get the wished dynamical control on the longitudinal shape of the FW (and at a certain extent on its transverse shape too).

2. *Theory of the "Dynamic Frozen Waves"* — Let us consider the time-dependent solution

$$\Psi(\rho, \phi, z, t) = \mathcal{N}_\nu \sum_{-N}^N A_n(t) J_\nu(k_{\rho n}(t) \rho) \exp(i\nu\phi) \exp(ik_{zn}(t) z) \exp(-i\omega t) \quad (2)$$

where one may recall that any expression of the type  $J_\nu(k_{\rho n}\rho) \exp(ik_{zn}z) \exp(-i\omega t)$ , with  $k_{\rho n}^2 + k_{zn}^2 = \omega^2/c^2$ , is a solution to the wave equation  $(\nabla^2 - 1/c^2 \partial_t^2)\Psi = 0$ . As already mentioned, in the case of slow temporal variations, we are able to obtain in the dynamical regime the longitudinal pattern  $F(z, t)$  and *either* the spot radius  $\Delta\rho_0(t)$  in the case of a zeroth-order FW; *or* the radius  $\rho_0(t)$  of the intensity cylindrical surface in the case of a higher order FW.

Namely: To obtain a dynamic FW, instead of  $F(z)$  we have to consider for  $0 \leq z \leq L$  a time-dependent function  $F(z, t)$ . Then, considering superposition (2), one can determine the coefficients  $A_n(t)$ :

$$A_n(t) = \frac{1}{L} \int_0^L F(z, t) e^{-i \frac{2\pi}{L} n z} dz, \quad (3)$$

with the time-variation of the longitudinal or transverse wave numbers  $k_{\rho n}(t) = \sqrt{(2\pi/\lambda)^2 - k_{zn}^2(t)}$  and  $k_{zn}(t) = Q(t) + 2\pi n/L$  depending on  $Q(t)$ ; which in its turn is linked either to the spot size  $\Delta\rho_0(t)$

$$Q(t) = \sqrt{k^2 - (2.4/\Delta\rho_0(t))^2} \quad (4)$$

in case of zero order FWs; or to the cylinder radius  $\rho_0(t)$

$$[(d/d\rho)J_\nu(\rho\sqrt{\omega^2/c^2 - Q^2(t)})]\Big|_{\rho=\rho_0(t)} = 0 \quad (5)$$

in case of higher order FWs.

We anticipated that a slow variation of  $F(z, t)$  and  $\Delta\rho_0(t)$  (or  $\rho_0(t)$ ), guarantees Eq.(2) to be an approximate solution to the wave equation. This can be shown by noting that for each term of the superposition (2) we have

$$\frac{\partial^2}{\partial t^2} [A_n(t) J_\nu(k_{\rho n}(t)\rho) \exp(ik_{zn}(t)z) \exp(-i\omega t)] \approx A_n(t) J_\nu(k_{\rho n}(t)\rho) \exp(ik_{zn}(t)z) \frac{\partial^2}{\partial t^2} \exp(-i\omega t). \quad (6)$$

The above approximation is valid due to the said slow variation, which implies that  $|\partial_t(A_n(t) J_\nu(k_{\rho n}(t)\rho) e^{ik_{zn}(t)z})| \ll |\omega A_n(t) J_\nu(k_{\rho n}(t)\rho)|$ . All this guarantees that Eq.(2) is a good approximate solution to the wave equation.

*3. Generation of Dynamic Frozen Waves (DFW): Experiments and results* — As already mentioned, the experimental holographic method for the generation of *static* FWs can be found in Refs.[8, 9]. Our present setup is shown in Fig.1. It is composed by an Argon ion laser (of 514,5 nm), which is expanded and collimated (Exp) in a nematic SLM device (LC R1080 SLM, HoloEye Photonics AG). We perform the amplitude modulation of a computer generated hologram (CGH) on the SLM by polarizer Pol and analyzer Anl, with angles 0° and 90°, respectively, measured with regard to the input SLM axis. The 4-f spatial *filtering* system[14, 8, 9] is used for the FW generation, the SLM (CGH) being placed at the input plane (focus of the first lens); while a spatial *filtering* mask (SF, *band-pass circular pupil*), located at the Fourier plane, *selects and transmits* the light from the initial spectrum, generating the encoded signal at the output plane of the setup. As a result, we get a propagation of the FW, whose intensity is registered with a CCD camera that can be displaced all along the distance  $0 < z < L$ .

Specifically, in the case of DFWs we discretized the relevant time interval (of 10 s, for instance) into  $m$  parts; and we obtained, for each value  $\tau_m$  of time, the coefficients of the series (3), and consequently the complex function  $\Psi(\rho, z, t = \tau_m)$  describing the FW at that instant of time. On knowing the field value at each time instant,  $m$  computer generated holograms (CGHs) are created. Then, by using a Spatial Light Modulator (SLM) linked to a microcomputer, the holograms are reproduced at a specific rate on the modulator display to get a reconstruction of the DFW: That is, of position and longitudinal (and transverse) shape, varying with time, of the dynamic frozen wave (see Fig.1). The LC-R1080 modulator possesses a rate of 70 Hz, enough for producing 15 frames per second.

The  $z$ -axis too is divided into  $j$  parts  $Z_j$ . The data acquisition is then performed leaving the CCD camera in the fixed position  $z_0 = 0$  (the beginning of the propagation axis), where all frames  $\tau_m$  reproduced by the SLM are captured; the process is repeated in the subsequent positions till the  $j$ -th one, as in Fig.2.

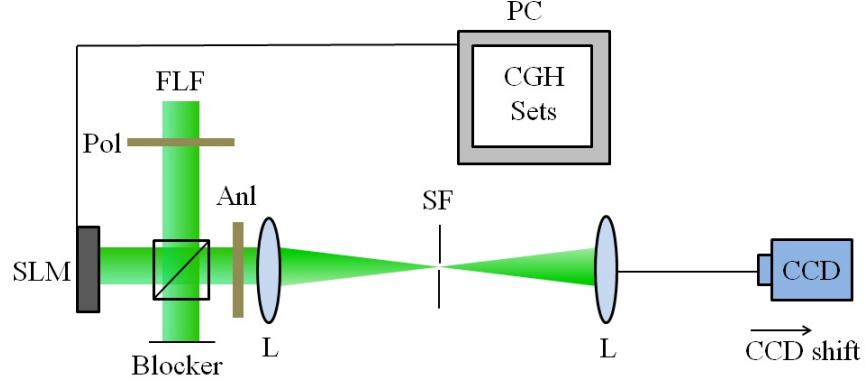


Figure 1: (color online) The experimental setup used for generating a dynamic Frozen Wave is essentially composed by an Argon ion laser beam, FLF being a beam collimator, Pol a polarizer, BS a beam splitter, SLM a nematic Spatial Light Modulator, and Anl an analyzer; while the L's are lenses, SF is a spatial filtering mask, and CCD is a camera for images/data acquisition.

3.1. First example (for a zeroth-order DFW): – Let us consider, in the space interval  $0 < z < L$ , an exponentially rising barrier of the type

$$F(z, t) = \begin{cases} \exp(Kzt), & \text{for } z_i \leq z \leq z_f \\ 0, & \text{elsewhere} \end{cases} \quad (7)$$

with  $z_i = z_0 + vt$  and  $z_f = \Delta D + z_0 - vt$ , quantity  $\Delta D = z_f - z_i$  being the width of the considered DFW at the initial time instant, and  $K^{-1} = 1 \text{ cm s}$ . The coefficients of our series, at each instant  $t$  of time, are given by Eq.(3) when inserting into it the function (7). Afterwards, the FW behavior in the considered time interval (e.g.,  $\Delta t = 10 \text{ s}$ ) is obtained by putting such values  $A_n(t)$  into solution (2).

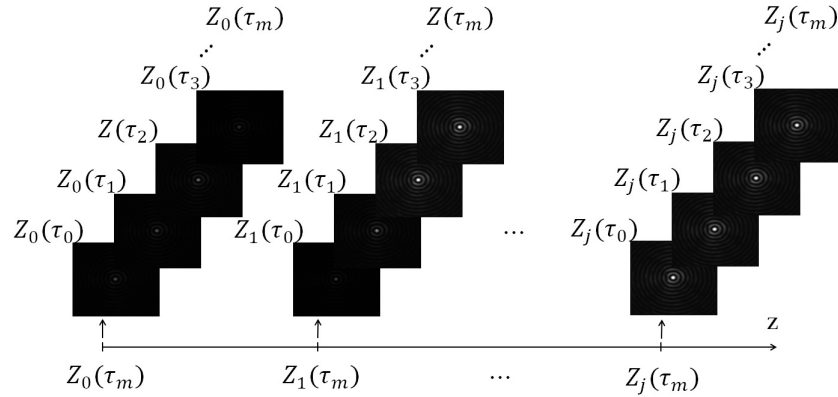


Figure 2: Scheme of the experimental data acquisition. The  $z$ -axis is divided into  $j$  parts  $Z_j$ ; the data acquisition is performed leaving the CCD camera in the fixed position  $z_0 = 0$ , where all frames  $\tau_m$  reproduced by the SLM are captured. The process is repeated in the subsequent positions till the  $j$ -th one.

Let us adopt the values:  $Q = 0.99997\omega/c$ , and  $L = 40 \text{ cm}$ , with  $N = 20$  superpositions; a step width  $\Delta D = 4 \text{ cm}$ ; initial position  $z_0 = 0.18 \text{ cm}$ , and finally a constant  $v = 1.3 \text{ cm/s}$ . The initial and final positions move with velocity  $-v$  and  $v$ , respectively. We then get a step profile which, as time elapses, modifies into the longitudinal exponential ramp expressed by Eq.(7). More specifically, let us

divide the time interval  $\Delta t = 10$  s into  $m = 150$  parts: From Eqs.(7) and (2) we obtain  $\Psi(\rho, z, t = \tau_m)$ , and for each time value  $\tau_m$  an amplitude hologram is generated, with a total of 150 holograms (frames).

In the present case, the  $z$ -axis was divided into 81 parts, and 143 frames were captured at each position  $Z(j)$ . This implies an error in the temporal reconstruction of the holograms (error due to the intrinsic limitations of the microcomputer hardware and of the software itself: think of the time spent by Matlab between command and execution) that can be evaluated to be of about 7%. In Figs.3 the longitudinal intensity profile for different time instants is shown, together with its corresponding orthogonal projections (while online, in “Media-1” the 3-D profile is shown in a dynamic way).

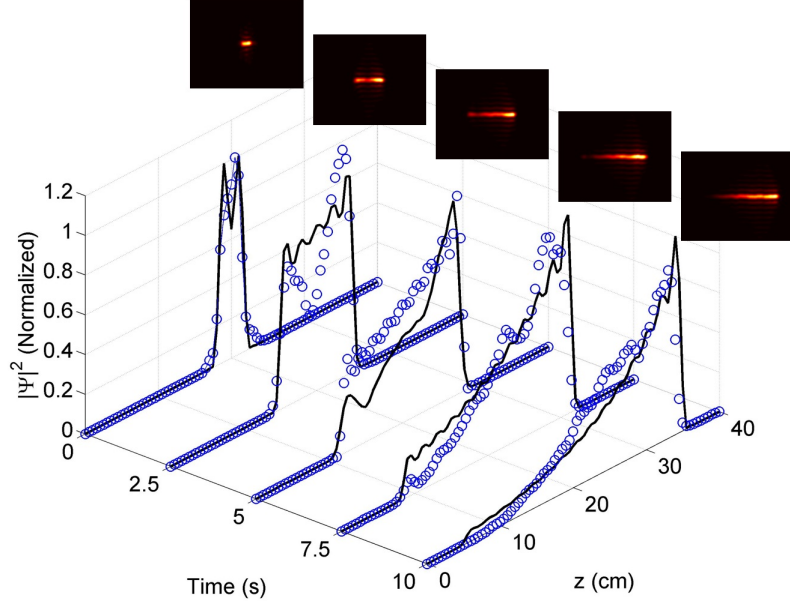


Figure 3: (color online) Time evolution (for  $\Delta t = 10$  s) of the longitudinal intensity pattern for the FW corresponding to the longitudinal intensity profile given by an exponentially rising ramp like (7). In the insets, the corresponding orthogonal projection are shown. See also Media-1 online.

3.2. Second example (for a first-order DFW): – We have presented above our experimental results for a dynamic FW of the zeroth order. The most intriguing cases are, however, the ones dealing with higher-order dynamic FWs. For the case of higher-order (static) FWs, in previous papers we theoretically constructed electromagnetic or acoustic *static envelopes* with the shape of donuts, or of cylindrical surfaces[11, 2, 7, 15]. Going on to higher-order DFWs, striking results appear: We present in our last Figure the experimental results referring to a first-order DFW, consisting in a cylindrical surface of light *whose geometry changes in space and in time*.

Our theoretical choice for a first-order DFW is as follows: We may theoretically construct a higher-order DFW, characterized by a duration  $T$ , whose behavior may be divided into three steps, with a duration  $T/3$  each, so that  $T_1 = T/3$  and  $T_2 = 2T/3$ ; and with a deformation speed (in each step) given by the alteration length divided by  $T/3$ . Namely, let us devise a FW initially consisting in a short cylindrical surface of length  $\Delta l_i$  and radius  $\rho_i$ , such that: (i) in the first step, the cylindrical surface is required to stretch, keeping its radius, till reaching the length  $\Delta l_f$ ; (ii) in the second step, the cylindrical surface keeps its length, but is requested to reduce continuously its radius, till the value  $\rho_f$ ; (iii) in the third step, the cylindrical surface —while keeping its radius  $\rho_f$ — is required to split into two cylinders, which become shorter till reaching the length  $\Delta l_f$  each.

Let us choose (for all steps) the simple function  $F(z, t)$  defined as zero everywhere (within  $0 < z < L$ ) except

$$F(z, t) = \begin{cases} 1 & \text{for } z_1 < z < z_2 \\ 1 & \text{for } z_3 < z < z_4, \end{cases} \quad (8)$$

depending on time through the values of  $z_1$ ,  $z_2$ ,  $z_3$  and  $z_4$ . Its radius will change in time according to  $Q = Q(t)$ .

To be more specific:

(i) *first movement*,  $0 < t < T_1 \equiv T/3$ : During this phase, the cylinder radius  $\rho_0 = \rho_i$  does not change, and the corresponding value of  $Q$  remains fixed, according Eq.(5). The  $z$  values are  $z_1 = z_{1i} - v_1 t$ ;  $z_2 = z_3 = z_{1i} + \Delta l_i / 2 \equiv \bar{z}$ ;  $z_4 = (z_{1i} + \Delta l_i) + v_1 t$ , that is,  $z_1$  and  $z_4$  change in time, while  $z_2$  and  $z_3$  remain fixed. The initial values of  $z_1$  and  $z_4$ , that we call  $z_{1i}$  and  $z_{4i} = z_{1i} + \Delta l_i$ , are still to be fixed; together with the final value  $z_{1f}$  of  $z_1$ , with  $z_1(T_1) = z_{1f} < z_{1i}$ , which also determines the final value of  $z_4$ , so that  $z_{4f} \equiv z_4(T_1) = (z_{1i} + \Delta l_i) + (z_{1i} - z_{1f})$ . The final length of the cylinder will be  $\Delta l_f = z_{4f} - z_{1f}$ , while the speed  $v_1$  will be  $v_1 = (z_{1i} - z_{1f})/T_1 = 3(z_{1i} - z_{1f})/T$ .

(ii) *second movement*,  $T_1 < t < T_2 \equiv 2T/3$ : The  $z$  values are the same assumed at time  $t = T_1$  in the previous step, that is,  $z_1 = z_{1f}$ ;  $z_2 = z_3 \equiv \bar{z}$ ;  $z_4 = z_{4f}$ ; but quantity  $Q$  will vary according to Eq.(5), where  $\rho_0(t) = \rho_i - v_2(t - T_1)$ . The final value of the radius,  $\rho_0(T_2) \equiv \rho_f$ , is still to be fixed, our request being merely that  $\rho_f < \rho_i$ . The speed  $v_2$  will be  $v_2 = (\rho_i - \rho_f)/(T_2 - T_1) = 3(\rho_i - \rho_f)/T$ .

(iii) *third movement*,  $T_2 < t < T_3 \equiv T$ : Quantity  $Q$  keeps constant and equal to the final value it acquired in the previous step. The  $z$  values will however change as follows:  $z_1 = z_{1f}$ ;  $z_2 = \bar{z} - v_3(t - T_2)$ ;  $z_3 = \bar{z} + v_3(t - T_2)$ ;  $z_4 = z_{4f}$ . The final value of  $z_2$  (and of  $z_3$ ) remains to be fixed, for instance through a choice for the final length ( $\Delta l_f$ ) of the two smaller cylinders: In fact, it will be  $z_2(T) = z_{1f} + \Delta l_f$ ; and, for the final value of  $z_3$ , one will have  $z_3(T) = z_{4f} - \Delta l_f$ . The speed is  $v_3 = (\bar{z} - z_2(T))/(T_3 - T_2) = 3(\bar{z} - z_2(T))/T$ .

This specifies all what is needed for the experimental creation of the devised higher-order (first order) DFW.

Its experimental production: — The experimental procedure is the one illustrated in the previous sections 2 and 3. For the definition interval of the DFW, that is,  $0 \leq z \leq L$ , it has been chosen the value  $L = 40$  cm, being the other parameters chosen as:  $T = 10$ s,  $z_{1i} = 0.18$  cm,  $z_{1f} = 0.05$  cm,  $\Delta l_i = 0.004$  cm,  $\rho_i = 35$   $\mu$ m and  $\rho_f = 25$   $\mu$ m. With this we have  $v_1 = 0.039$ m/s,  $v_2 = 3$  $\mu$ m/s and  $v_3 = 0.03$ m/s. As to Eq.(2), the value  $N = 12$  has been adopted.

In Figs.4 the experimental results are shown of the time evolution, during  $\Delta t = 10$  s, of the intensity pattern for our first-order dynamic FW; as well as the orthogonal projections of the corresponding cylindrical surfaces. The final radius of the cylindrical surface has been chosen to be  $\rho_f = 25$   $\mu$ m, and its initial radius results to be  $\rho_i = 35$   $\mu$ m. Noticeably, as time elapses, the cylindrical surface stretches its length (while narrowing its radius), and afterwards splits into two short cylinders: see also Media-2 online.

4. *Conclusions* — The Non-Diffracting Waves (NDW) are solutions to the (linear) wave equation which travel well confined (*localized*), in a single direction, and with other interesting properties like self-healing. The Frozen Waves (FW) are NDWs with zero peak-velocity, i.e. with a static envelope, whose longitudinal intensity pattern can be freely modeled —both theoretically and experimentally— within a prefixed space interval of the propagation axis. In this paper we present, first, the theory of “dynamic FWs” (DFW) whose shape is now allowed to slightly evolve in time in a predetermined way, and, second, their experimental generation by holographic techniques (namely, by a holographic setup along with an optical reconstruction of dynamic holograms CGHs by using a LC-SLM). The most interesting

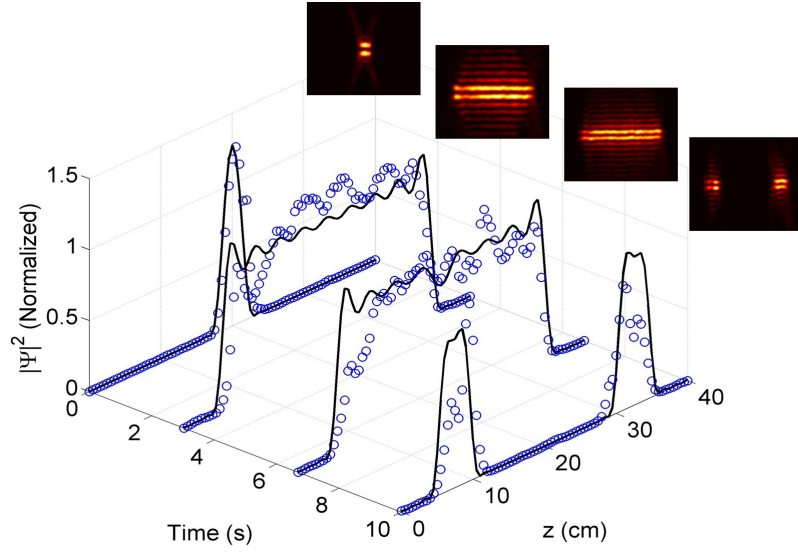


Figure 4: (color online) Time evolution, during  $\Delta t = 10$  s, of the intensity pattern for our first-order dynamic FW; and orthogonal projections of the corresponding cylindrical surfaces: *experimental results*. The final radius of the cylindrical surface has been chosen to be  $\rho_f = 25 \mu$ , and its initial radius results to be  $\rho_i = 35 \mu$ . Noticeably, as time elapses, the cylindrical surface stretches its length (while narrowing its radius), and afterwards splits into two shorter cylinders: See also Media-2 online.

experimental results, depicted in our last Figure (and in movies online), refer to the higher-order FW consisting in a cylindrical surface of light whose radius changes in space and time. We show that, as time elapses, the cylindrical surface stretches its length (while narrowing its radius), and afterwards splits into two shorter cylinders. The experimental results are in agreement with the theoretical predictions, and open exciting possibilities of generating many further potentially interesting DFWs for scientific and technological applications.

## References

- [1] M.Zamboni-Rached, Opt. Express **12**, 4001 (2004).
- [2] M.Zamboni-Rached, E.Recami, and H.E.Hernández-Figueroa, Journal of the Optical Society of America **A22**, 2465 (2005).
- [3] M.Zamboni-Rached, Opt. Express **14**, 1804 (2006).
- [4] J.Durnin, T.J.Miceli, and J.H.Eberly, Phys. Rev. Lett. **58**, 708 (1993).
- [5] P.Saari, and K.Reivelt, Phys. Rev. Lett. **97**, 4135 (1997).
- [6] E.Recami et al., IEEE Journal of Selected Topics in Quantum Electronics **9**, 59 (2003).
- [7] M.Zamboni-Rached, L.A.Ambrosio, and Hugo E.Hernández Figueroa, Applied Optics **49**, 5861 (2010).
- [8] T.A.Vieira, M.R.R.Gesualdi, and M.Zamboni-Rached, Optics Letters **37**, 2934 (2012).
- [9] T.A.Vieira, M.Zamboni-Rached and M.R.R.Gesualdi, Opt. Commun. **315**, 374 (2014).

- [10] L.J.Prego-Borges, M.Zamboni-Rached, H.E.Hernández-Figueroa, and E.Recami, IEEE Trans. Ultrason. Ferroel. Freq. Control **60**, 2414 (2013).
- [11] H.E.Hernández-Figueroa, M.Zamboni-Rached, and E.Recami (editors), *Localized Waves* (J.Wiley, Hoboken, NJ, 2008).
- [12] H.E.Hernández-Figueroa, E.Recami, and M.Zamboni-Rached (editors), *Non-Diffracting Waves* (J.Wiley-vch, Berlin, 2014).
- [13] A.Vasara, J.Turunen, and A.Friberg: J. Opt. Soc. Am. **A6**, 1748 (1989).
- [14] V.Arrizón, Opt. Letters **28**, 2521 (2003).
- [15] E.Recami, M.Z.Rached, H.E.H.Figueroa, et al., "Method and Apparatus for Producing Stationary (Intense) Wavefields of arbitrary shape", USA PATENT no. US-2011/0100880-A1, publication date 05/05/11: granted (owned by Bracco Imaging, Spa).